doi:10.4149/neo_2021_210607N762

LDLR promotes growth and invasion in renal cell carcinoma and activates the EGFR pathway

Gui-Ming ZHANG[1,2,*], Wei CHEN[1], Yu YAO[1], Lei LUO[1], Li-Jiang SUN[1]

[1]*Department of Urology, The Affiliated Hospital of Qingdao University, Qingdao, China;* [2]*Department of Urology, Fudan University Shanghai Cancer Center, Shanghai, China*

**Correspondence: zhangguiming9@126.com*

Received June 7, 2021 / Accepted October 26, 2021

Previous studies identified an association of low-density lipoprotein (LDL) levels and LDL receptor (LDLR) with renal cell carcinoma (RCC) development. This study investigated the expression and roles of LDLR in RCC. LDLR expression was examined in clear cell RCC (ccRCC) and adjacent normal kidney tissues, and its clinicopathological significance was analyzed. The role of LDLR in RCC cell proliferation, cell cycle, and invasion were assessed in RCC cells with LDLR stable knockdown. LDLR expression was higher in ccRCC tissues than in normal kidney tissues and increased with RCC progression. LDLR knockdown in RCC cells inhibited cell growth, migration and invasion, and induced G1/S cell cycle arrest. We identified an interaction between LDLR and EGFR, and EGFR signaling protein expression was reduced after LDLR knockdown. Our findings reveal that LDLR plays an important role in RCC carcinogenesis, suggesting that LDL and LDLR might be potential targets for therapeutic intervention in RCC.

Key words: renal cell carcinoma, low-density lipoprotein receptor, cell proliferation, invasion, EGFR

Renal cell carcinoma (RCC) represents 2–3% of all malignancies, with a peak incidence between 50 and 70 years of age [1]. Over the past two decades, RCC has increased in incidence by about 2%, and the incidence is higher in developed countries such as Europe and North America than in Asia and Africa [2]. Both genetic background and environmental factors contribute to RCC carcinogenesis. Although the real etiology of RCC remains unknown, altered lifestyle factors, obesity, and hypertension are thought to be responsible in part for RCC development [3].

Recent studies have proposed that RCC might be a metabolic disorder, as metabolic syndrome (MS) is reported to be associated with an increased RCC risk [4]. MS comprises a cluster of metabolic abnormalities, each of which has been linked with altered RCC risk and exhibits insulin resistance as the common trait. Obesity and hypertension have been listed as confirmed etiological factors in the guidelines of the American Urological Association, the European Association of Urology, and the Chinese Urological Association. Furthermore, diabetes also has a close relationship with RCC. Lindblad and colleagues found that both morbidity and mortality of RCC increased in patients with diabetes compared with the general population [5]. In addition, the RCC genes identified so far are involved in pathways that respond to nutrient stimulation and/or metabolic stress [6]. For example, clear cell RCC (ccRCC), the main histological type of RCC, is commonly associated with a genetic mutation in the von Hippel-Lindau (*VHL*) gene [7], and the VHL complex is a component of the oxygen and iron sensing pathway that regulates hypoxia-inducible factor (HIF) levels [6]. Therefore, targeting these fundamental metabolic abnormalities in RCC might provide a novel approach for the treatment of this disease.

Increasing studies have investigated the role of dyslipidemia, a predominant component of MS, in the initiation and development of cancers. ccRCC is characterized by sterol storage in cancer cells, which prompts an abnormality in cell lipid metabolism. Horiguchi et al. found that fluvastatin, a type of statin that is an effective drug for dyslipidemia, inhibited RCC cell growth, invasion, angiogenesis, and metastasis *in vitro* [8]. Our previous study examined the prevalence of dyslipidemia in RCC patients in a Chinese population, and we observed that abnormal low-density lipoprotein (LDL) elevation was common in RCC cases compared with controls [9]. We further explored the association between LDL receptor (LDLR) polymorphism and ccRCC risk and found that functional variants in the *LDLR* gene are associated with ccRCC susceptibility [10]. Therefore, we speculated

that LDLR might be involved in ccRCC carcinogenesis. In this study, we examined the expression of LDLR in ccRCC tissues and explored its association with clinicopathological characteristics. Furthermore, the impact of LDLR on RCC cell growth and invasion was also investigated.

Patients and methods

Patient samples. A total of 574 consecutive ccRCC patients who underwent surgical treatment between January 2010 and December 2013 at the Department of Urology, Fudan University Shanghai Cancer Center (FUSCC) were enrolled in this study. Tumor tissues and adjacent normal kidney tissues were obtained after surgery and stored in the FUSCC Tissue Bank. All patients were diagnosed with ccRCC based on histopathological evaluation and did not receive radiotherapy, chemotherapy, or targeted therapy before surgery. Clinicopathological information of all patients, including age, sex, body mass index (BMI), smoking status, history of hypertension and diabetes, Fuhrman grade, and TNM staging (based on the Union for International Cancer Control, 7th edition, 2009), was acquired from medical records. The Institutional Research Review Boards of FUSCC approved this study protocol and written informed consent was obtained from all participants. All procedures performed in studies involving human participants were in accordance with the ethical standards of the institutional and/or national research committee and with the 1964 Helsinki declaration and its later amendments or comparable ethical standards. This study is approved by the Ethics Committee of Fudan University Shanghai Cancer Center.

Cell culture. Five human RCC cell lines (ACHN, 786-O, A498, 769-P, Caki-1) were obtained from the Institute of Cell Research of the Chinese Academy of Sciences (Shanghai, China). The ACHN and Caki-1 cell lines were grown in MEM and McCoy's 5A medium (Gibco; Thermo Fisher Scientific, Inc., USA), respectively, and the 786-O, A498, and 769-P cell lines were cultured in RPMI-1640 medium (Hyclone; GE Healthcare Life Sciences, Logan, USA). All media were supplemented with 10% fetal bovine serum, 100 U/ml penicillin, and 100 μg/ml streptomycin (Hyclone; GE Healthcare Life Sciences, USA), and cells were maintained at 37 °C in a humidified atmosphere containing 5% CO_2.

Immunohistochemistry (IHC). LDLR protein expression was detected by IHC on 5 μm thick tissue sections prepared from formalin-fixed, paraffin-embedded tissue from a constructed 10×12 tissue microarray that was made by the FUSCC Tissue Bank, as described previously [11]. After deparaffinization, dehydration, antigen retrieval, and endogenous peroxidase activity blocking, tissue sections were incubated with antibody against LDLR (Santa Cruz Biotechnology, Santa Cruz, USA) (sc18823) and SABC (goat IgG) detection kit (BOSTER, Wuhan, China). The IHC staining results were independently scored by two pathologists who were blinded to patient information.

RNA extraction and quantitative real-time PCR. Total RNA from tissues and cultured cells was extracted using TRIzol reagent. Single-stranded cDNA was synthesized with the RevertAid First Strand cDNA Synthesis Kit (Life Technology, Carlsbad, USA). Real-time PCR was performed using the SYBR Green PCR Master Mix (Applied Biosystems, Foster City, USA). The fold change of LDLR gene expression was determined using β-actin mRNA level as an internal control. Primer sequences were as follows: LDLR-F: TCTGCGAGGGACCCAACAAG, LDLR-R: TCGTTGGTCCCGCACTCTTT; and β-actin F: ACCGAGCGCGGCTACAG, β-actin R: CTTAATGTCACGCACGATTTCC.

Western blotting. Total protein was isolated from tissues and cells using RIPA lysis buffer, and protein concentration was quantified by the BCA assay kit (Thermo Fisher Scientific, Waltham, USA) according to the manufacturer's protocol. Protein samples (50 μg) were separated by 10% SDS polyacrylamide gel electrophoresis and transferred to nitrocellulose membranes. The membranes were first blocked and then incubated with primary antibodies overnight at 4 °C. After washing with phosphate-buffered saline (PBS), membranes were incubated with horseradish peroxidase (HRP)-conjugated secondary antibodies (Santa Cruz Biotechnology, Santa Cruz, USA), and proteins were visualized using an ECL detection system (Thermo Fisher Scientific, USA). The primary antibodies were purchased from Santa Cruz Biotechnology (Santa Cruz, USA) or Abcam Company (Abcam, Cambridge, UK) as follows: LDLR (sc18823), EGFR (sc53274), Cyclin D1 (sc8396), mTOR (sc517464), pAKT (sc81433), GAPDH (sc32233), β-tubulin (sc5274), CDK4 (ab68266), $p21^{Cip1}$ (ab188224), $p27^{Kip1}$ (ab62364), AKT (ab8805), S6K (ab32359), p-S6K (ab59208), Ras (ab52939).

Vector construction and lentivirus production and infection. Short hairpin RNA (shRNA) for LDLR was introduced into the pLKO.3G vector and transfected into HEK293T cells along with psPAX2 and PMD2-G using Lipofectamine 2000 reagent (Life Technology, Carlsbad, USA) according to the manufacturer's protocol. Forty-eight hours later, lentivirus was harvested and used to infect RCC cells. Puromycin (2 μg/ml) was added into the medium to select stable infected cell clones. The efficiency of LDLR knockdown was confirmed by qRT-PCR and western blotting. The sequences of LDLR and control shRNAs are listed in Supplementary Table S1.

Cell proliferation and colony formation assays. CCK-8 assay (Dojindo, Shanghai, China), EdU assay (Ribobio, Guangzhou, China), and colony formation assay were performed to measure cell proliferation. For CCK-8 assays, cells were seeded in 96-well plates (4×10^3 cells/well) and cultured for 24 h. Next, 10 μl of CCK-8 solution was added to each well, and cells were incubated for another 2 h. The absorbance values were measured at 450 nm using a microplate reader. For EdU assays, cells were incubated in the EdU solution (1:5000) for 2 h, harvested, and washed using PBS mixed with TritonX-100 (200:1). Cells were then stained

with the Cell-Light EdU Apollo 643 In Vitro Flow Cytometry Kit according to the manufacturer's protocol and analyzed by flow cytometry (Beckman Coulter, USA). For colony formation assays, a total of 600 cells were seeded in a 6-well plate in triplicate per experimental group and cultured at 37 °C in a 5% CO_2 incubator for 14 days. The medium was replaced with 4% paraformaldehyde (1 ml/well) and cells were incubated for 60 min at room temperature. After removing the supernatant, the clones were stained using 0.5% crystal violet for 30 min and counted under a light microscope.

***In vivo* tumorigenicity.** All animal studies were approved by the Animal Studies Ethics Committee of FUSCC. BALB/c nude mice were purchased from Shanghai SLAC Laboratory Animal Co., Ltd. ACHN-LDLR-shRNA or ACNH-Scr cells (1×10^7/ml cells) were implanted subcutaneously in both sides of the back region of nude mice. Tumor sizes were measured at least three times a week. At week 5 after injection, mice were euthanized with CO_2 and the tumors were removed. Tumor weight was examined and tumor volume was calculated after sacrificing.

Cell cycle and apoptosis assays. Cell cycle and apoptosis assays were both performed using flow cytometry (Beckman Coulter, USA). Briefly, cells were cultured for 72 h at 37 °C, washed with PBS three times, and then fixed with 75% ethanol overnight at 4 °C. Propidium iodide (50 μg/ml) containing RNase was added to the cells for DNA staining. Stained cells were subjected to flow cytometry for cell cycle analysis. For cell apoptosis assays, cells were resuspended in 100 μl buffer containing Annexin V; next, 5 μl FITC-Annexin V and 5 μl propidium iodide (BD Biosciences, Franklin Lakes, USA) were added to cells for staining. After incubating at room temperature in the dark for 15 min, 400 μl of binding buffer was added to each cell suspension, and cells were subjected to analysis by flow cytometry.

Cell migration and invasion assays. Wound-healing assay and Transwell chamber assay were performed to test cell migration and invasion *in vitro*, respectively. For wound-healing assays, cells were seeded in a monolayer in 6-well plates. A scratch was introduced in the cell monolayer in the middle of each well using a 200 μl pipette tip. Images of cells were captured under an inverted microscope at 0 and 24 h time points. For migration assays, a total of 4×10^4 cells were seeded into the upper chamber of a Transwell chamber (BD Biosciences, Franklin Lakes, USA) coated with 60 μl Matrigel (BD Biosciences, Franklin Lakes, USA) diluted with serum-free medium (1:50), and 600 μl of medium supplemented with 10% FBS was added to the lower chamber. After incubation for 24 h, cells were fixed with 4% polyoxymethylene and stained with crystal violet. Cells on the upper surface of the membrane were wiped off with cotton swabs, and those that invaded through the pores were photographed and counted using an inverted microscope in five random fields.

Immunofluorescence. Cells were seeded on coverslips overnight and then fixed with 4% paraformaldehyde for 30 min. After incubating in 1% BSA and 0.25% Triton X-100 in PBS, cells were incubated with EGFR antibody (sc53274) or LDLR antibody (sc18823) (Santa Cruz Biotechnology, Santa Cruz, USA) at room temperature, followed by the incubation with Alexa Fluor 594 IgG donkey anti-rabbit antibody (Invitrogen, Carlsbad, USA) for 1 h at room temperature. Nuclei detection was performed using DAPI co-staining. Fluorescence images were acquired with a laser confocal microscope.

Co-immunoprecipitation. Cells were washed with PBS and lysed using RIPA buffer containing protease inhibitors (Roche Diagnostics, Basel, Switzerland). Protein samples were incubated with specific antibodies overnight at 4 °C and then 50 μl beads (Santa Cruz Biotechnology, Santa Cruz, USA) were added to the mixture. Samples were then incubated at 4 °C for 4 h. The beads were washed in ice-cold PBS, re-suspended in loading buffer, and incubated at 90 °C for 10 min. After separation on a 10% Bis-Tris gel, the samples were analyzed by western blot analysis.

Statistical analyses. All data are presented as means ± standard deviation. Student's t-test was used to compare the statistical differences between variables. All statistical analyses were performed using SPSS software version 20.0 (IBM SPSS, Armonk, USA), and two-sided $p<0.05$ was considered to indicate a statistically significant difference.

Results

LDLR expression levels in ccRCC tissues. We examined the expression of LDLR in ccRCC tissues and kidney tissues using IHC. Tumor tissues were acquired from 286 ccRCC patients, and adjacent normal kidney tissues were available for 188 patients. The clinicopathological characteristics of the 286 patients are listed in Supplementary Table S2. The mean (±SD) patient age was 55.8±12.2 years. There were 157 patients with Fuhrman I–II (low-grade) and 129 patients with Fuhrman III–IV (high-grade) disease. The expression levels of LDLR were classified into strongly-positive, weakly-positive, and negative groups according to IHC staining (Figures 1A–1F). Strongly-positive, weakly-positive, and negative staining were observed in 181, 92, and 13 ccRCC tissues and in 90, 89, and 9 normal kidney tissues, respectively. LDLR expression was higher in ccRCC tissues than in normal kidney tissues ($p<0.05$, Figure 1G). In addition, strongly-positive, weakly-positive, and negative staining were observed in 90, 59, and 8 low-grade ccRCC tissues and in 91, 33, and 5 in high-grade tissues, respectively. LDLR expression was higher in high-grade tissues than in low-grade tissues, however with a marginal statistical significance ($p=0.069$, Figure 1H).

We also detected the mRNA expression of LDLR in a different set of 288 ccRCC tissues and 100 adjacent normal kidney tissues. Supplementary Table S3 lists the clinicopathological features of these 288 patients. Of the 288 patients, 135 presented with Fuhrman I–II (low-grade) and 153 with Fuhrman III–IV (high-grade) disease, while 246 presented with stage I–II and 42 presented with stage III–IV disease.

LDLR mRNA expression was significantly higher in high-grade and stage III–IV diseases compared with low-grade and stage I–II diseases, respectively ($p<0.05$, Figures 1J, 1K). Interestingly, we observed lower expression of LDLR in ccRCC tissues than in normal kidney tissues ($p<0.05$, Figure 1I).

Validation of LDLR knockdown in RCC cells. To explore the biological function of LDLR in RCC, we first measured the protein and mRNA expression levels of LDLR in five human RCC cell lines (ACHN, 786-O, A498, 769-P, and Caki-1). We observed relatively high expression of LDLR in ACHN and 786-O cells at both mRNA and protein levels (Figures 2A, 2B). We selected ACHN cells for subsequent knockdown experiments.

Using lentivirus-mediated shRNA expression, we downregulated the expression of LDLR in ACHN cells. The knockdown efficiencies of the shRNAs are shown in Figure 2C. Compared with control shRNA, shRNA1 reduced the levels of LDLR. We chose this construct to establish stable knockdown cells (named ACHN-LDLR-shRNA) for further experiments.

Effects of LDLR knockdown on RCC cell proliferation. We used CCK8, EdU, and colony-forming assays to investigate the effects of LDLR knockdown on RCC cell proliferation *in vitro*. As demonstrated in Figures 3A and 3C, cell growth was significantly inhibited in ACHN-LDLR-shRNA cells compared with relevant controls ($p<0.05$), as shown by both CCK8 and EdU assays. In addition, compared with controls,

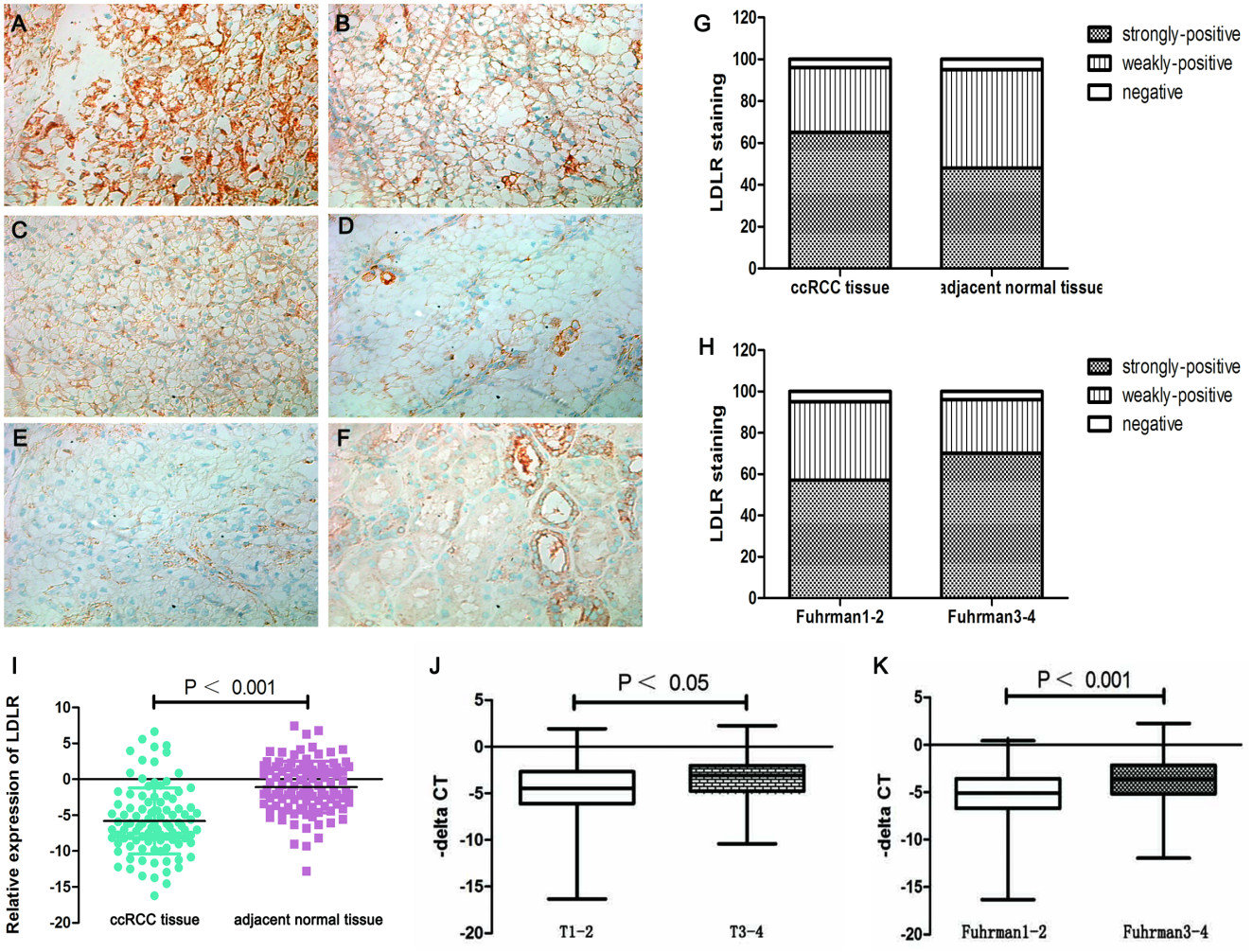

Figure 1. LDLR expression levels in ccRCC tissues and normal kidney tissues. (A–H) IHC staining (400×): A) Fuhrman 4 grade; B) Fuhrman 3 grade; C–E) Fuhrman 2 grade; F) adjacent normal kidney tissue; A, B) strongly-positive; C, D) weakly-positive; E) negative; F) negative expression in proximal convoluted tubules and positive expression in distal convoluted tubules; G) schematic representation of different LDLR expression in ccRCC tissues and adjacent normal kidney tissue; H) schematic representation of different LDLR expression in low-grade and high-grade ccRCC tissues; I) lower expression of LDLR mRNA in ccRCC tissues compared with normal kidney tissues ($p<0.001$); J) higher expression of LDLR mRNA in stage III–IV diseased compared with stage I–II diseases ($p<0.05$); K) higher expression of LDLR mRNA in Fuhrman 3–4 diseased compared with Fuhrman 1–2 diseases ($p<0.001$).

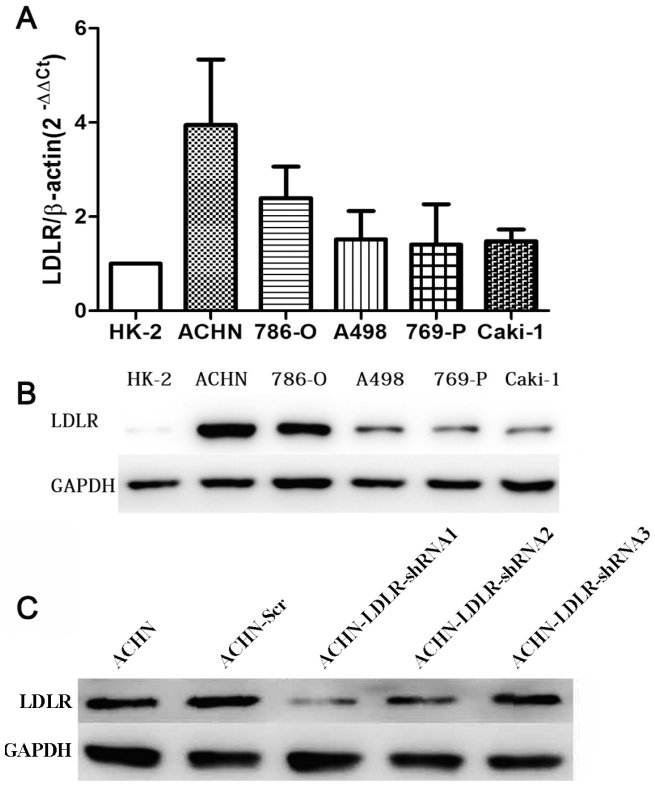

Figure 2. LDLR expression profiles in human RCC cell lines and LDLR knockdown ACHN cells. LDLR mRNA and protein expression was detected in five human RCC cell lines by RT-PCR (A) and western blot (B); C) Lower expression of LDLR was detected in LDLR knockdown ACHN cells using western blot.

ACHN-LDLR-shRNA cells developed fewer colonies at day 14 in colony formation assays ($p<0.05$, Figure 3B). Taken together, these results revealed that LDLR knockdown exerted a suppressive role on RCC cell proliferation *in vitro*.

To examine whether LDLR knockdown also affects RCC cell growth *in vivo*, subcutaneous tumor models were established in five nude mice using ACHN-LDLR-shRNA or control cells. The mice were sacrificed on day 38 after injection. We found that both tumor volume and mass were notably lower in ACHN-LDLR-shRNA tumors than in controls ($p<0.05$, Figures 3D–3F). Together, these results demonstrated that downregulated LDLR expression inhibited cell proliferation in RCC cells both *in vitro* and *in vivo*.

Effects of LDLR knockdown on RCC cell migration and invasion. A would-healing assay was used to evaluate the effect of LDLR knockdown on cell migration and a Transwell assay was performed to detect the invasiveness of RCC cells with LDLR knockdown. As shown in Figures 4A–4D, cell migration of ACHN-LDLR-shRNA cells was markedly reduced 24 h after wound creation. Transwell assays demonstrated that LDLR knockdown significantly inhibited the invasive capacity of ACHN cells compared with the control cells (Figures 4E, 4F). These observations indicate that LDLR knockdown restrains the migration and invasion abilities of RCC cells.

Effects of LDLR knockdown on RCC cell cycle and apoptosis. As LDLR knockdown exerts an inhibitory effect on RCC cell proliferation, we further explored its role in the cell cycle and cell apoptosis. Compared with controls, ACHN-LDLR-shRNA cells showed a notable increase in the G1 phase population, while the proportion of cells in the S phase decreased (Figures 4G, 4H), indicating that LDLR knockdown induced a G1/S cell cycle arrest. This arrest was accompanied by elevated expression of $p21^{Cip1}$ and $p27^{Kip1}$ as well as decreased expression of cyclin D1 and CDK4 (Figure 5C). However, we did not observe obvious differences in cell apoptosis between ACHN-LDLR-shRNA cells and controls (data not shown).

Effects of LDLR knockdown on the EGFR pathway. To further investigate the mechanisms by which LDLR affects RCC carcinogenesis, we performed mass spectrometry, co-immunoprecipitation, and immunocytofluorescence analyses to identify the proteins that interact with LDLR. As shown in Figures 5A and 5B, an interaction between LDLR and EGFR was observed. EGF and EGFR, which belong to a growth factor signaling pathway, are important participants in cancer initiation and development. We thus examined several important proteins in the EGFR signaling pathway. As indicated in Figure 5D, the expression levels of EGFR, mTOR, AKT, pAKT, p-S6K, and Ras were all reduced after LDLR knockdown compared with controls.

Discussion

The prevalence of obesity and obesity-related chronic diseases has dramatically increased worldwide over the past decades. Besides cardiovascular disease (CVD) and diabetes, common cancers investigated in the context of obesity include breast, colorectal, prostate, and endometrial cancers, as well as RCC [12]. Haggstrom et al. explored metabolic factors associated with RCC risk and found that obesity, hypertension, and dyslipidemia contribute to an increased RCC risk [13]. Based on studies suggesting that abnormal lipid metabolism may play a role in the biological process driving RCC development, we examined the expression and role of LDLR, an important molecule involved in cholesterol homeostasis, in ccRCC and found that the levels of LDLR were elevated with the progression of RCC. Downregulation of LDLR in RCC cells remarkably inhibited cell proliferation, migration, and invasion and induced G1/S cell cycle arrest. Additionally, we observed an interaction between LDLR and EGFR, suggesting that LDLR may promote growth and invasion in RCC by activating the EGFR pathway.

LDLR is a ubiquitously expressed cell membrane glycoprotein that binds and internalizes circulating cholesterol-containing lipoprotein particles. LDLR is an essential mediator for lipid metabolism, and its dysfunction has been

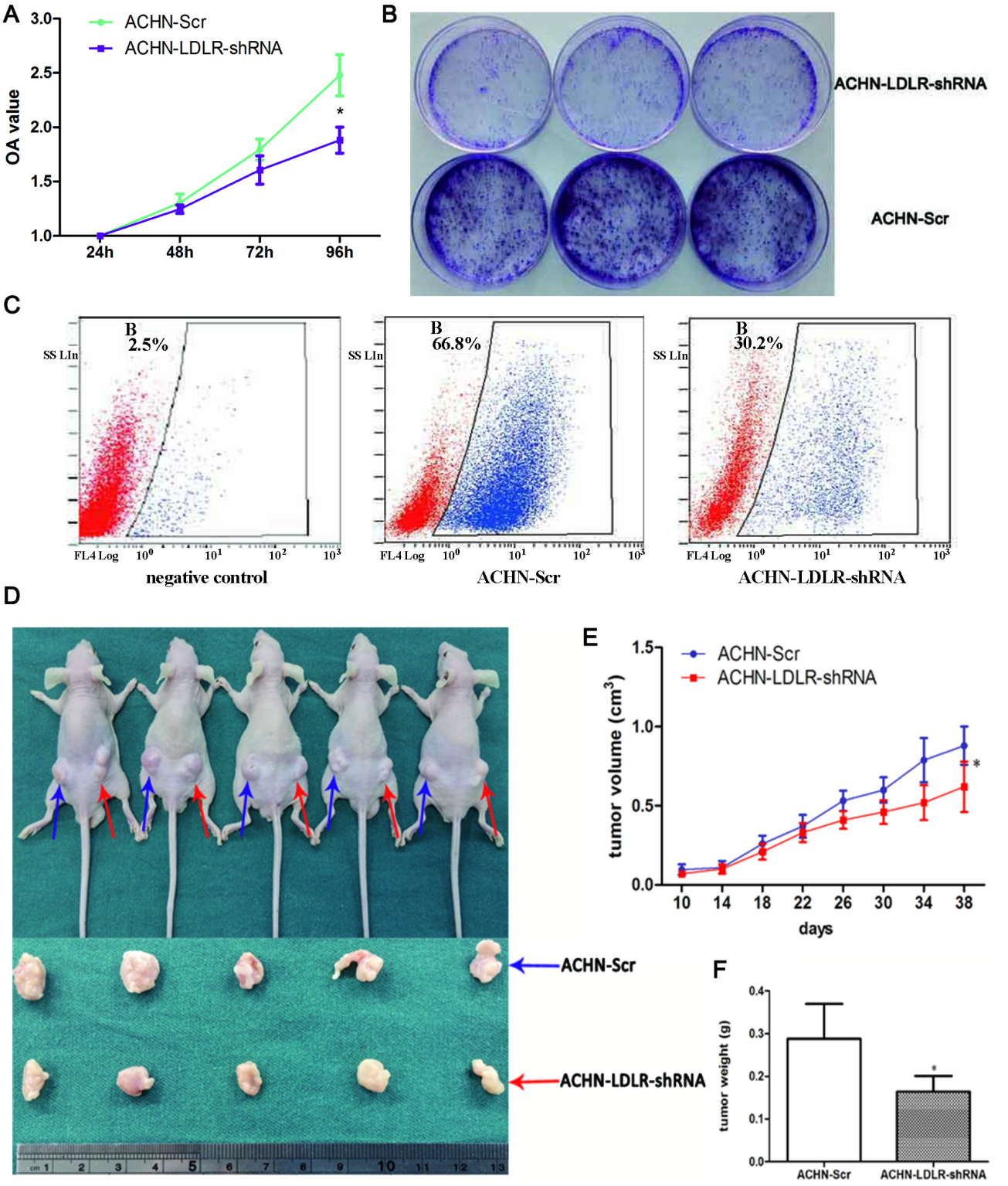

Figure 3 LDLR knockdown significantly inhibits cell growth in RCC cells *in vitro* and *in vivo*. A) The CCK-8 assay was used to examine cell proliferation in LDLR knockdown ACHN cells and controls. Data represent the mean ± SD of the optical density value detected at 450 nm from three independent experiments; B) Colony formation assays indicated fewer colonies in LDLR knockdown ACHN cells; C) Cell proliferation was detected in ACHN-LDLR-shRNA and controls using EdU assay and analyzed by flow cytometry; D) ACHN-Scr and ACHN-LDLR-shRNA cells were injected into the left and right posterior flank of nude mice, respectively; The tumor volume (E) and mass (F) in the ACHN-LDLR-shRNA group were significantly lower than in the ACHN-Scr group (*$p<0.05$).

proven to contribute to familial hypercholesterolemia and early-onset coronary heart disease [14, 15]. Previous genome-wide association studies have reported that LDLR genetic susceptibility is associated with serum lipid levels [16–18]. However, relatively few studies to date have investigated the role of LDLR in cancer development. Rudling et al. observed relatively lower mRNA expression of LDLR in RCC tissues compared with normal kidney tissues [19]. Consistent with Rudling's results, we also observed lower LDLR expression at the mRNA level in RCC tissues compared with normal kidney tissues. Interestingly, our IHC results showed the opposite phenomenon: LDLR expression was higher in ccRCC tissues than in normal kidney tissues. We speculate that this discrepancy might be attributed to different sampling processes. IHC staining was judged in the area of proximal convoluted tubules from where ccRCC is derived. However, the tissue ultrastructure was not separated when mRNA was tested. Hence, the LDLR mRNA levels reflected levels expressed in both distal and proximal convoluted tubules. Notably, in tumor tissues, LDLR expression was higher in high-grade disease than in low-grade disease at both mRNA and protein levels. In addition, LDLR mRNA expression was significantly higher in stage III–IV diseases compared with stage I–II diseases. Therefore, we speculate that LDLR exerts a role in promoting RCC development.

In breast cancer patients, a higher level of intratumor cholesteryl ester displayed a higher expression of LDLR at both mRNA and protein levels and was linked to cell proliferation and aggressive tumor potential [20]. Gallagher et al. used mouse models for hyperlipidemia and publicly available human datasets to determine the importance of LDLR in breast cancer. The authors found that silencing LDLR in breast cancer cells led to decreased growth of Her2Neu-overexpressing tumor cells both *in vitro* and *in vivo*, and high LDLR expression in human breast cancers was associated with decreased recurrence-free survival [21]. In our study, we observed similar roles of LDLR in ccRCC, suggesting that LDLR might be a contributing factor in obesity-related cancers. However, Gallagher et al. also found that LDLR knockdown resulted in increased caspase 3 cleavage. In mice lacking LDLR, increased

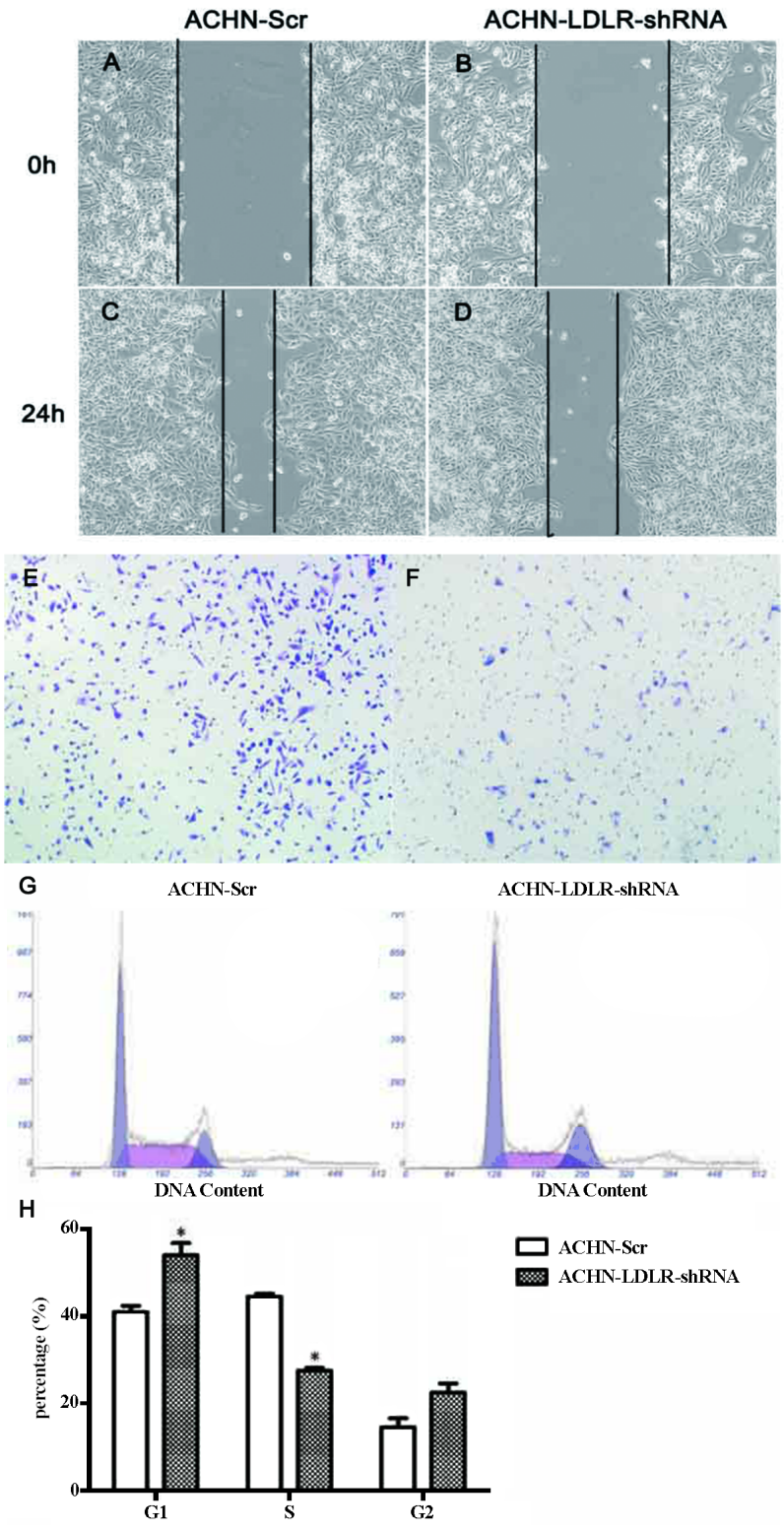

Figure 4. LDLR knockdown restrains the migration and invasion abilities and induced a G1/S cell cycle arrest in RCC cells. A–D) Wound-healing assay showed markedly reduced cell migration in ACHN-LDLR-shRNA cells; E, F) Transwell assays demonstrated significantly inhibited invasive capacity in LDLR knockdown cells; G, H) LDLR knockdown induced a G1/S cell cycle arrest in ACHN cells.

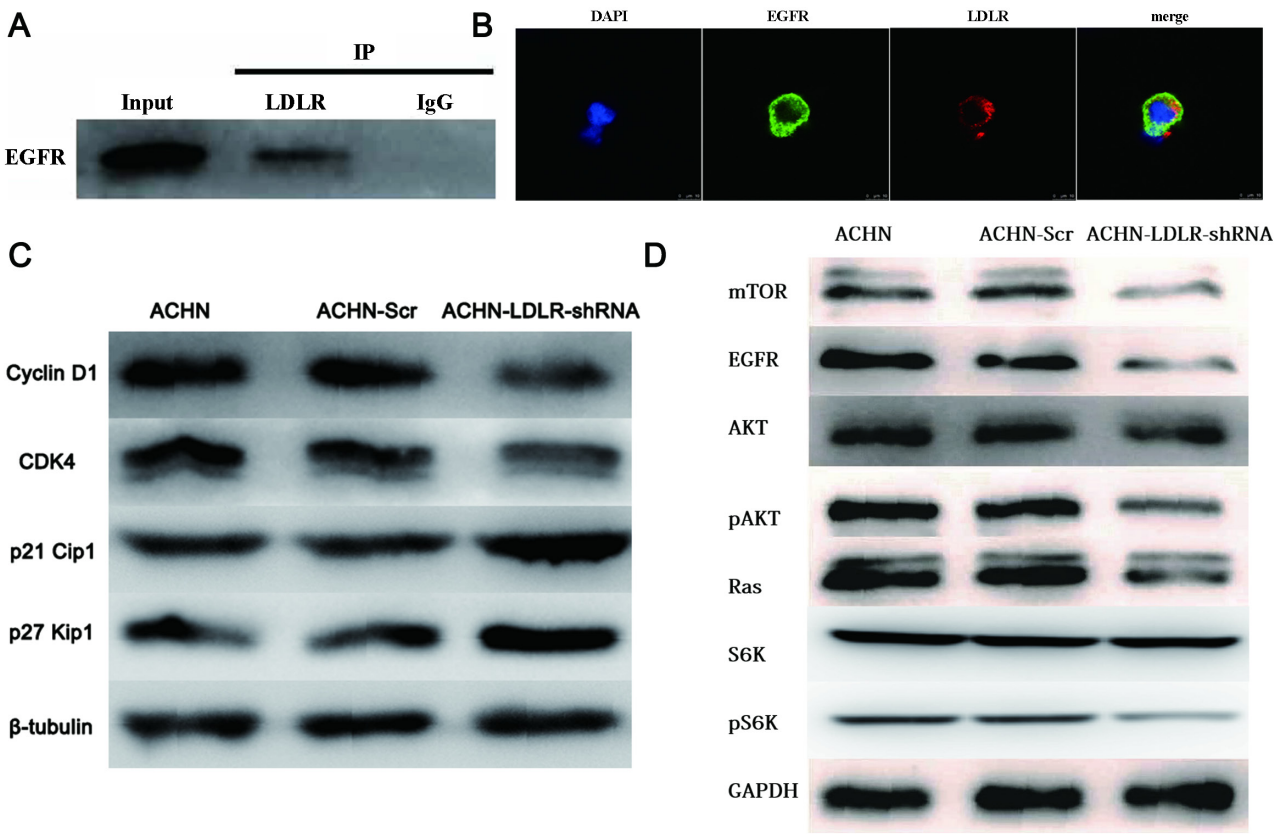

Figure 5. Interaction between LDLR and EGFR and effects of LDLR knockdown on EGFR pathway. An interaction between LDLR and EGFR was observed using co-immunoprecipitation (A) and immunocytofluorescence analyses (B); LDLR knockdown triggered alterations in cell cycle-related molecules (C), and the EGFR signaling pathway (D).

cell apoptosis was also observed in the liver [22]. We did not observe an association between LDLR knockdown and RCC cell apoptosis. Tumor heterogeneity may account for this discrepancy. In addition, we did not perform follow-up because most of our subjects were with early-stage diseases. Further investigations are needed to explore the complete mechanisms and clinical effects of LDLR in RCC.

Increasing evidence has revealed the important role of growth factor-related signaling pathways in cancer initiation and progression. Among these pathways, EGF-EGFR is a key signaling pathway and its abnormal activity has been observed in many cancers, including breast, lung, esophageal, colorectal, head and neck cancers [23]. The EGF-EGFR pathway participates in tumor cell proliferation, apoptosis, migration, invasion, and angiogenesis as well as the pathogenesis of many renal disorders [24, 25]. Stumm et al. reported that EGFR is overexpressed in RCC and is associated with tumor initiation and progression [26]. Therefore, although some EGFR inhibitors such as gefitinib and erlotinib have shown therapeutic outcomes that are less than expected, targeting the EGFR signaling pathway is still an attractive and promising intervention in cancer therapy. In our study, we identified EGFR as a binding partner of LDLR and confirmed that LDLR interacted with EGFR. We further showed that LDLR knockdown led to decreased expressions of EGFR, mTOR, AKT, pAKT, and Ras. These results suggest that LDLR might promote RCC growth and invasion by activating the EGFR signaling pathway. To date, several new drugs targeting EGFR and/or related signaling molecules have been tested for application in RCC [27, 28]. However, the deeper mechanism underlying the cross-talk between LDLR and EGFR, as well as the therapeutic effect of new compounds targeting the LDLR signaling pathway, still remains to be explored.

In conclusion, our results revealed that LDLR promotes RCC cell growth and invasion through activating the EGFR signaling pathway. This study provides another clinical implication. Dyslipidemia is an important risk factor in the development of CVD, and recent studies have identified some cardiovascular biomarkers that are associated with RCC progression [29]. Thus, we speculate that CVD may share etiology with RCC, and we might benefit more from better control of abnormal lipid profiles.

Supplementary information is available in the online version of the paper.

Acknowledgments: We thank Liwen Bianji, Edanz Editing China (www.liwenbianji.cn/ac), for editing the English text of a draft of this manuscript. This study was partly funded by the National Natural Science Foundation of China (Grant No. NSFC 81502195) and the Clinical Medicine + X Project of The Affiliated Hospital of Qingdao University (No. QDFY+X2021029).

References

[1] BRAY F, FERLAY J, SOERJOMATARAM I, SIEGEL RL, TORRE LA et al. Global cancer statistics 2018: GLOBOCAN estimates of incidence and mortality worldwide for 36 cancers in 185 countries. CA Cancer J Clin 2018; 68: 394–424. https://doi.org/10.3322/caac.21492

[2] LJUNGBERG B, BENSALAH K, CANFIELD S, DABESTANI S, HOFMANN F et al. EAU guidelines on renal cell carcinoma: 2014 update. Eur Urol 2015; 67: 913–924. https://doi.org/10.1016/j.eururo.2015.01.005

[3] CHOW WH, GRIDLEY G, FRAUMENI JF JR, JARVHOLM B. Obesity, hypertension, and the risk of kidney cancer in men. N Engl J Med 2000; 343: 1305–1311. https://doi.org/10.1056/NEJM200011023431804

[4] ZHANG GM, ZHU Y, YE DW. Metabolic syndrome and renal cell carcinoma. World J Surg Oncol 2014; 12: 236. https://doi.org/10.1186/1477-7819-12-236

[5] LINDBLAD P, CHOW WH, CHAN J, BERGSTROM A, WOLK A et al. The role of diabetes mellitus in the aetiology of renal cell cancer. Diabetologia 1999; 42: 107–112. https://doi.org/10.1007/s001250051122

[6] LINEHAN WM, SRINIVASAN R, SCHMIDT LS. The genetic basis of kidney cancer: a metabolic disease. Nat Rev Urol 2010; 7: 277–285. https://doi.org/10.1038/nrurol.2010.47

[7] BARONTINI M, DAHIA PL. VHL disease. Best Pract Res Clin Endocrinol Metab 2010; 24: 401–413. https://doi.org/10.1016/j.beem.2010.01.002

[8] HORIGUCHI A, SUMITOMO M, ASAKUMA J, ASANO T, ASANO T et al. 3-hydroxy-3-methylglutaryl-coenzyme a reductase inhibitor, fluvastatin, as a novel agent for prophylaxis of renal cancer metastasis. Clin Cancer Res 2004; 10: 8648–8655. https://doi.org/10.1158/1078-0432.ccr-04-1568

[9] ZHANG GM, ZHU Y, LUO L, ZHANG HL, GU CY et al. Prevalence of dyslipidaemia in patients with renal cell carcinoma: a case-control study in China. BJU Int 2014; 113: E75–E81. https://doi.org/10.1111/bju.12581

[10] ZHANG GM, WANG MY, LIU YN, ZHU Y, WAN FN et al. Functional variants in the low-density lipoprotein receptor gene are associated with clear cell renal cell carcinoma susceptibility. Carcinogenesis 2017; 38: 1241–1248. https://doi.org/10.1093/carcin/bgx098

[11] SHI TY, YANG G, TU XY, YANG JM, QIAN J et al. RAD52 variants predict platinum resistance and prognosis of cervical cancer. PLoS One 2012; 7: e50461. https://doi.org/10.1371/journal.pone.0050461

[12] MELVIN JC, HOLMBERG L, ROHRMANN S, LODA M, VAN HEMELRIJCK M. Serum lipid profiles and cancer risk in the context of obesity: four meta-analyses. J Cancer Epidemiol 2013; 2013: 823849. https://doi.org/10.1155/2013/823849

[13] HAGGSTROM C, RAPP K, STOCKS T, MANJER J, BJORGE T et al. Metabolic factors associated with risk of renal cell carcinoma. PLoS One 2013; 8: e57475. https://doi.org/10.1371/journal.pone.0057475

[14] BROWN MS, GOLDSTEIN JL. A receptor-mediated pathway for cholesterol homeostasis. Science 1986; 232: 34–47.

[15] CIVEIRA F, INTERNATIONAL PANEL ON MANAGEMENT OF FAMILIAL H. Guidelines for the diagnosis and management of heterozygous familial hypercholesterolemia. Atherosclerosis 2004; 173: 55–68. https://doi.org/10.1016/j.atherosclerosis.2003.11.010

[16] SANDHU MS, WATERWORTH DM, DEBENHAM SL, WHEELER E, PAPADAKIS K et al. LDL-cholesterol concentrations: a genome-wide association study. Lancet 2008; 371: 483–491. https://doi.org/10.1016/S0140-6736(08)60208-1

[17] KATHIRESAN S, WILLER CJ, PELOSO GM, DEMISSIE S, MUSUNURU K et al. Common variants at 30 loci contribute to polygenic dyslipidemia. Nat Genet 2009; 41: 56–65. https://doi.org/10.1038/ng.291

[18] WATERWORTH DM, RICKETTS SL, SONG K, CHEN L, ZHAO JH et al. Genetic variants influencing circulating lipid levels and risk of coronary artery disease. Arterioscler Thromb Vasc Biol 2010; 30: 2264–2276. https://doi.org/10.1161/ATVBAHA.109.201020

[19] RUDLING M, COLLINS VP. Low density lipoprotein receptor and 3-hydroxy-3-methylglutaryl coenzyme A reductase mRNA levels are coordinately reduced in human renal cell carcinoma. Biochim Biophys Acta 1996; 1299: 75–79.

[20] DE GONZALO-CALVO D, LOPEZ-VILARO L, NASARRE L, PEREZ-OLABARRIA M, VAZQUEZ T et al. Intratumor cholesteryl ester accumulation is associated with human breast cancer proliferation and aggressive potential: a molecular and clinicopathological study. BMC Cancer 2015; 15: 460. https://doi.org/10.1186/s12885-015-1469-5

[21] GALLAGHER EJ, ZELENKO Z, NEEL BA, ANTONIOU IM, RAJAN L et al. Elevated tumor LDLR expression accelerates LDL cholesterol-mediated breast cancer growth in mouse models of hyperlipidemia. Oncogene 2017; 36: 6462–6471. https://doi.org/10.1038/onc.2017.247

[22] BIEGHS V, VAN GORP PJ, WOUTERS K, HENDRIKX T, GIJBELS MJ et al. LDL receptor knock-out mice are a physiological model particularly vulnerable to study the onset of inflammation in non-alcoholic fatty liver disease. PLoS One 2012; 7: e30668. https://doi.org/10.1371/journal.pone.0030668

[23] SESHACHARYULU P, PONNUSAMY MP, HARIDAS D, JAIN M, GANTI AK et al. Targeting the EGFR signaling pathway in cancer therapy. Expert Opin Ther Targets 2012; 16: 15–31. https://doi.org/10.1517/14728222.2011.648617

[24] CHUNG H, RAMACHANDRAN R, HOLLENBERG MD, MURUVE DA. Proteinase-activated receptor-2 transactivation of epidermal growth factor receptor and transforming growth factor-beta receptor signaling pathways contributes to renal fibrosis. J Biol Chem 2013; 288: 37319–37331. https://doi.org/10.1074/jbc.M113.492793

[25] ZHANG MZ, WANG Y, PAUEKSAKON P, HARRIS RC. Epidermal growth factor receptor inhibition slows progression of diabetic nephropathy in association with a decrease in endoplasmic reticulum stress and an increase in autophagy. Diabetes 2014; 63: 2063–2072. https://doi.org/10.2337/db13-1279

[26] STUMM G, EBERWEIN S, ROSTOCK-WOLF S, STEIN H, POMER S et al. Concomitant overexpression of the EGFR and erbB-2 genes in renal cell carcinoma (RCC) is correlated with dedifferentiation and metastasis. Int J Cancer 1996; 69: 17–22. https://doi.org/10.1002/(SICI)1097-0215(19960220)69:1<17::AID-IJC4>3.0.CO;2-Z

[27] SONG W, DANG Q, XU D, CHEN Y, ZHU G et al. Kaempferol induces cell cycle arrest and apoptosis in renal cell carcinoma through EGFR/p38 signaling. Oncol Rep 2014; 31: 1350–1356. https://doi.org/10.3892/or.2014.2965

[28] ROWINSKY EK, SCHWARTZ GH, GOLLOB JA, THOMPSON JA, VOGELZANG NJ et al. Safety, pharmacokinetics, and activity of ABX-EGF, a fully human anti-epidermal growth factor receptor monoclonal antibody in patients with metastatic renal cell cancer. J Clin Oncol 2004; 22: 3003–3015. https://doi.org/10.1200/JCO.2004.11.061

[29] KAMAI T, TOKURA Y, UEMATSU T, SAKAMOTO K, SUZUKI I et al. Elevated serum levels of cardiovascular biomarkers are associated with progression of renal cancer. Open Heart 2018; 5: e000666. https://doi.org/10.1136/openhrt-2017-000666